Annual Progress Report for JFY 2005

March 15, 2006

# CDF Experiment

Spokespersons
Japan S. Kim (University of Tsukuba)
U.S.A. Y. K. Kim (University of Chicago) and R. Roser (Fermilab)

The year 2005 marked the fifth year for the Tevatron Run-II program and the CDF Run-II experiment, which officially started in March 2001. The Tevatron accelerator has been operational with 36 bunches of protons and anti-protons, respectively, at an increased center-of-mass energy of 1.96 TeV. The improvement in the accelerator performance seen in years 2003 and 2004 continued in 2005. Recently a typical peak luminosity is $\mathcal{L} = 1.5 \times 10^{32}$ cm$^{-2}$ s$^{-1}$, with a record luminosity of $1.8 \times 10^{32}$ cm$^{-2}$ s$^{-1}$ (Figure 1(top)). The latter has surpassed the Run-IIa goal of $8.6 \times 10^{31}$ cm$^{-2}$ s$^{-1}$. A weekly integrated luminosity in excess of 20 pb$^{-1}$ has also been achieved several times. The total integrated luminosity in the calendar year 2005 is about 800 pb$^{-1}$, more than twice that of 2004, and the Run II total is roughly 1.6 fb$^{-1}$ (Figure 1(bottom)).

The upgraded CDF detector has been functioning very well with high efficiency. The integrated luminosity recorded by CDF amounts to roughtly 1.2 fb$^{-1}$, more than ten times that of Run I (Figure 2). We expect to collect 2 fb$^{-1}$ by the end of 2006, 4 fb$^{-1}$ in 2007, and 8 fb$^{-1}$ in 2009.

For operations at a high luminosity, CDF needs further upgrades to some of the detector components, in particular the DAQ system that allows efficient data taking and data logging. They include the upgrades to the silicon-based trigger system (SVT) and to the consumer server/logger system (CS/L).

In the remainder of this report we summarize physics results and prospects, and detector upgrade efforts, with an emphasis on contributions from the Japan group.

## 1 Physics Results and Prospects in Run II

We expect a data sample corresponding to an integrated luminosity of 2 fb$^{-1}$ in the very near future. This is a twenty-fold increase in the amount of data over the previous run,

Run I. Also, the Tevatron beam energy has been increased to give a center-of-mass energy of 1.96 TeV.

We plan on carrying out a broad physics program, and many important physics results have already emerged from Run-II data. We describe some of them below, along with prospects in the near future.

## 1.1 Electroweak physics

Studies of single gauge boson production continue, at a new center of mass energy of 1.96 TeV. Clean signals of $W^+ \to \ell^+\nu$ and $Z^0 \to \ell^+\ell^-$ decays have been observed in Run-II data, including the candidates where the decay electrons are detected in the forward region with the plug calorimeter.

Figure 3 shows transverse mass distribution of the lepton (electron and muon) and missing transverse energy system for $W^\pm \to \ell^\pm\nu$ candidates from a data set corresponding to 200 pb$^{-1}$ of data. These events will be used for $W$ boson mass measurements, where a total uncertainty of about 70 MeV/$c^2$ is expected.

With 2 fb$^{-1}$ of data the $W^\pm$ boson mass will be measured with a precision of about 30 MeV/$c^2$. Combined with top quark mass measurements, it will provide constraints on the Higgs boson mass with a relative precision of 30%.

## 1.2 Top quark properties

Since the top quark was discovered by CDF in 1995 in Run-I data, tens of pair-produced top quark events were reconstructed and various measurements of their properties were performed in a data sample of 110 pb$^{-1}$. However, most of them were statistically limited, given the relatively small number of the reconstructed events. Therefore, all measurements are expected to improve with the increased amount of data in Run II, and some have already achieved that goal already.

The top analysis with Run-II data has produced results on measurements of the mass and production cross section using various decay channels. The production cross section has been measured using both lepton + jet and di-lepton channels. A candidate event in the lepton + jet channel is shown in Figure 4, where two $b$-jets are identified by secondary vertex tags. The jet multiplicity distribution of the $b$-tagged $W + n$-jet events is shown in Figure 5, where the excess over expected background in $n = 3$ and $n \geq 4$ bins is explained by the contributions from the top quark. The $t\bar{t}$ production cross section is measured to be $\sigma = 8.2 \pm 0.6 \pm 1.0$ pb with this channel [1]. The corresponding cross section from the di-lepton channel is $\sigma = 8.3 \pm 1.5 \pm 1.1$ pb [2]. They both are in agreement with a next-to-leading order QCD calculation of $6.7^{+0.71}_{-0.88}$ pb for $m_{\rm top} = 175$ GeV/$c^2$.

The top quark mass is extracted using various techniques, both from the lepton + jet channel and the dilepton channel. K. Sato and T. Tomura (Tsukuba) have used the lepton

+ jet channel and applied the looser second $b$-jet tagging method called "jet probability tags" in addition to the tigher "SECVTX" tags. Tagging two $b$-quark jets is particularly important in mass measurements, because it reduces not only the background but also the number of combinations that have to be considered in a given $t\bar{t}$ event. The reconstructed mass distribution is shown in Figure 6 (top), and the extracted mass value is $m_{\rm top} = 173.5\,^{+\,3.7}_{-\,3.6}$ (stat) $\pm\,1.3$ (syst) GeV/$c^2$ (320 pb$^{-1}$) [3]. Understanding the energy scale of calorimeters for hadronic jets is a crucial component for this measurement. It has been achieved by reconsrcting the $W$ boson mass using $W \to q\bar{q}$ candidates in the $t\bar{t}$ events themselves. This is shown in Figure 6 (bottom). K. Sato finished his Ph.D. research with the subject [4].

Another very precise measurement of the top quark mass comes from the analysis of the events in the same channel using the Dynamical Likelihood Method [5]. It utilizes maximal information such as subprocess matrix elements and parton distributions. The reconstructed mass distribution is shown in Figure 7 (top), and the extracted mass value is $m_{\rm top} = 173.2\,^{+\,2.6}_{-\,2.4}$ (stat) $\pm 3.2$ (syst) GeV/$c^2$ (320 pb$^{-1}$) [3, 6]. K. Yorita (Waseda) performed this analysis for his Ph.D. thesis [7]. R. Tsuchiya (Waseda) applied the same method to the top quark candidates in the dilepton channel, and measured the top quark mass to be $m_{\rm top} = 166.6\,^{+\,7.3}_{-\,6.7}$ (stat) $\pm\,3.2$ (syst) GeV/$c^2$ using 340 pb$^{-1}$ of data [8]. The reconstructed mass distribution is shown in Figure 7 (bottom).

When combined with the measurements with the D0 experiment, the top quark mass as of summer 2005 is $m_t = 172.7 \pm 2.9$ GeV/$c^2$. The precision has already surpassed the Run-II (2 fb$^{-1}$) goal of 3 GeV/$c^2$ [9], and is beginning to constrain the Higgs boson mass significantly (Figure 8).

Other production and decay properties will be also measured precisely, including $t\bar{t}$ spin correlations and $W^{\pm}$ boson helicity. Y. Takeuchi (Tsukuba) has been working on spin correlations using the dilepton channel, and expects to obtain a preliminary result soon. Single top quark production should be observed as we accumulate more data, which should allow a direct measurement of the partial width $\Gamma(t \to W^+ b)$ and a determination of CKM matrix element $|V_{tb}|$ to about 13%. Also, searches have been performed and will be continued for new particles such as a charged Higgs boson through the top decay $t \to H^+ b$, and for new resonant states decaying into $t\bar{t}$ pairs.

## 1.3 Quantum chromodynamics

A wide variety of measurements are being made at a new center-of-mass energy of 1.96 TeV. Also, increased statistics allow measurements in a wider range of spectra, e.g. highest $E_T$ jets, photons and other objects, and with less statistical uncertainties. They will serve as precision tests of perturbative QCD calculations.

An example is a measurement of the production cross sections of $J/\psi$'s. In Run I, CDF found a surprisingly high rate of direct production of $J/\psi$'s, fifty times higher than

theory [10]. The lowered muon trigger threshold has provided a reasonable acceptance down to $p_T^{J/\psi} = 0$. The production cross section is measured as a function of $p_T^{J/\psi}$. The value integrated over $p_T$ and rapidity $|y| < 0.6$ is $240 \pm 1 \,^{+35}_{-28}$ nb [11]. The sample should also allow a better measurement of production polarization, which is very useful in discriminating various production mechanisms, such as gluon fragmentation and color octet models.

An investigation of decay length distributions of $J/\psi$'s provides a discrimination of the sources of $J/\psi$'s, namely prompt production vs. $B \to J/\psi$. The latter contribution has been determined over the nearly full kinematic range, and thus enabled a measurement of the (almost) total $b$-quark production cross section for the first time. The result is $\sigma(\bar{p}p \to bX; p_T^b > 0, |y^b| < 1.0) = 29.4 \pm 0.6 \pm 6.2$ $\mu$b [11]. This has helped understnad the long-standing puzzle of a possible excess of $b$-quark production rates over next-to-leading order QCD calculations.

T. Yamashita (Okayama) has contributed to the $J/\psi$ production analyses and obtained his Ph. D. degree [12].

## 1.4 Bottom and charm physics

Traditionally CDF relied on leptons to trigger on and collect decays of $B$ hadrons, such as $\bar{B} \to \ell^- \bar{\nu} X$ and $B \to J/\psi X \to \ell^+ \ell^- X$. In Run II, CDF has introduced a device called SVT, which uses information from the silicon vertex detector at the second level of the trigger and calculates impact parameter of charged particle tracks with a resolution of about 50 $\mu$m for $p_T > 2$ GeV/$c$. It enables us to collect decay products of long-lived particles such as $B$ and charm hadrons.

Lepton triggers are effective and useful channels for $B$ physics. Figure 9 shows di-muon signals in Run-II data. Various resonance states, such as $J/\psi \to \mu^+\mu^-$ and $\Upsilon \to \mu^+\mu^-$, are observed cleanly. Thanks to a lowered $p_T$ threshold on muons, $J/\psi$ yield per recorded luminosity is a factor of two higher than in Run I. Various $B$-hadron signals such as $B^+ \to J/\psi K^+$, $B^0 \to J/\psi K^{*0}$, $B^0 \to J/\psi K_S^0$, $B_s^0 \to J/\psi\,\phi$ and $\Lambda_b^0 \to J/\psi\,\Lambda^0$ have been observed and are used to measure their masses, lifetimes and relative branching fractions. Also, the FCNC decays $B_d^0/B_s^0 \to \mu^+\mu^-$ decays have been looked for, and the most stringent limits are set on their branching fractions.

M. Aoki (Tsukuba) has worked on the $B_c^-$ ($\equiv b\bar{c}$) meson reconstruction using the semileptonic decay $B_c^- \to \ell^- \bar{\nu} J/\psi X$. Figure 10 (top) shows the mass distribution of the $J/\psi\, e^-$ pairs, where a signal of about 115 events is observed onver the estimated backgrounds. The production rate, relative to the similar production and decay chain $b \to B^- X \to (J/\psi K^-)\, X$, is measured to be $0.282 \pm 0.038 \pm 0.035 \pm 0.065$. These events are also used to extract the lifetime of the $B_c^-$ meson, using their decay length distribution (bottom). The measured lifetime is $\tau(B_c^-) = 0.474\,^{+0.073}_{-0.066} \pm 0.033$ ps [13]. M. Aoki obtained his Ph.D. with the analyses.

Single leptons are a good sample to collect and study semileptonic decays of $B$ hadrons. S. Uozumi (Tsukuba) has been a major contributor in this area. The previous analysis

provided a high-statistics measurement of the lifetimes of the $B^-$ and $\bar{B}^0$ mesons using the decays $\bar{B} \to \ell^- \bar{\nu} D^0 X$ and $\bar{B} \to \ell^- \bar{\nu} D^{*+} X$. The analysis has been extented to the $\bar{B}_s^0$ meson, using the decays $\bar{B}_s^0 \to \ell^- \bar{\nu} D_s^+ X$. Their signal is shown in Figure 11, as well as their decay length distribution. The $B_s^0$ meson lifetime has been measured to be $\tau(B_s^0) = 1.381 \pm 0.055\,^{+0.052}_{-0.046}$ ps, and the ratio to the $B_d^0$ meson lifetime to be $\tau(B_s^0)/\tau(B_d^0) = 0.938 \pm 0.044\,^{+0.049}_{-0.046}$. An attempt to measure the width difference between the mass eigenstates of the $B_s^0$-$\bar{B}_s^0$ system is being made. S. Uozumi has obtained his Ph.D. with the analyses [14].

One of the primary $B$ physics goals at CDF is to observe $B_s^0 \overline{B}_s^0$ oscillations and measure its frequency $\Delta m_s$. It should provide a determination of the Cabibbo-Kobayashi-Maskawa matrix elements $|V_{td}/V_{ts}|$ with less model-dependent way. This is a crucial test of the unitarity triangle of the CKM matrix. CDF uses fully reconstructed decays collected with SVT so as to allow precise determination of $B_s^0$ meson momentum on an event-by-event basis. For a modest value of $\Delta m_s$, the partially reconstructed semileptonic decays $\bar{B}_s^0 \to \ell^- \bar{\nu} D_s^+ X$ are also useful. Such signals have also been observed, which are shown in Figure 12. To look for possible $B_s^0$-$\bar{B}_s^0$ oscillations, an amplitude analysis has been employed. This is shown in Figure 13, where the amplitude of the oscillations is shown as a function of the oscillation frequency $\Delta m_s$. From the data points, we exclude the region $\Delta m_s < 8.6$ ps$^{-1}$ with a sensitivity of 13 ps$^{-1}$.

## 1.5 New particle searches

Searches for the Higgs boson, supersymmetric particles and other new particles have been performed. Cross sections for the standard model Higgs boson production at the Tevatron is shown in Figure 14 (top) for various subprocesses. The largest contribution comes from the single production through gluon fusion, with the top quark in the loop. Associatied production with weak bosons $W^{\pm}H$ and $Z^0H$ are smaller. The decay branching fractions of the Higgs boson are shown in Figure 14 (bottom). At a low mass, say below 120 GeV/$c^2$, the decay to $b\bar{b}$ pairs is dominant, while at high mass the decays to weak boson pairs become dominant.

Thus far CDF has searched for the Higgs boson production in three different final states. The first, aimed at a low mass Higgs, looks for the associated production $\bar{p}p \to VHX$, where $V$ is a weak gauge boson $W^{\pm}$ or $Z^0$, with the $W^{\pm}$ ($Z^0$) boson decaying into $\ell^{\pm}\nu$ ($\nu\bar{\nu}$) pairs, and the Higgs boson to $b\bar{b}$ pairs. The $b$ quark jets are identified with displaced vertices. The main background comes from heavy flavor production in association with the $W$ boson, and top quark pair production. The number of events as well as the di-jet mass distribution (Figure 15) are examined for possible production of the Higgs boson. No excess is found and upper limits on the Higgs boson production is set at roughly one order of magnitude larger than the standard model predictions [15]. Y. Ishizawa (Tsukuba) completed his Ph.D. with the search [16].

The second analysis looks for the single production of the Higgs boson followed by its

decays to $W$ boson pairs. The channel is sensitive for high mass Higgs. The $W^+W^-$ final state is identified with their decays to leptons, thus two energetic leptons and large missing transverse energy and nothing else. The dominant background is the electroweak $W^+W^-$ production, which leads to the same signature. However, there exists a difference in the lepton azimuthal angle correlations in the two processes. Again, no excess of events is observed and upper limits on Higgs production have been placed.

The third method looks for associated production of the Higgs boson with a weak boson $W^{\pm}$ or $Z^0$, where the Higgs boson decays to $W^+W^-$ boson pair and one or both of the $W$ boson can be off mass shell. There exist three weak bosons in the final state, where two of them have the same charge. They are required to decay leptonically, leading to a distinctive final state of isolated, same-charge lepton pairs, such as $e^+\mu^+$. No candidate event is observed in the search region and upper limits on production cross sections are placed [17]. H. Kobayashi (Tsukuba) has performed the analysis.

The results from the three analyses are summarized in Figure 16, where the obtained upper limits on cross sections are compared to standard model predictions. The limits are larger than the predictions by an order of magnitude, and an increase in the amount of data is crucial.

# 2 Detector Operations and Upgrades

## 2.1 Detector operations

The original upgrades to the CDF detector for Run II have been completed for a few years now. The involvement and contributions of the Japan group included :

- plug calorimeter (Tsukuba)
- silicon detectors SVX-II (Hiroshima, Okayama) and ISL (Tsukuba, Osaka City)
- data acquisition system : consumer server/logger (Tsukuba, Nagasaki), silicon vertex trigger (Tsukuba), and online monitoring (Waseda)
- muon detector system (Waseda)
- time-of-flight counters (Tsukuba)
- silicon detectors for Run-IIb (Tsukuba, Okayama)
- central calorimeter preshower detector (Tsukuba)

Now that the experiment is in a stable data-taking mode, the detector activities have mostly shifted to daily operations and monitoring.

However, there are still activities for further upgrades of the detector designed for expected increase in the Tevatron luminosity. We describe them here in the following subsections.

## 2.2 Consumer server/logger

M. Shimojima (Nagasaki), and H. Matsunaga and T. Akimoto (Tsukuba) have been responsible for the consumer-server/logger system, which, as part of the online data acquisition system, receives events from the level-3 trigger and sends to disk and tape storage devices as well as to online monitoring programs. In the original design of the system, the data transfer rate is 20 MB/s (or 80 events per second) and it has been achieved. However, with the recent improvements in the accelerator luminosity and the further increase anticipated in the near future, this rate would not be sufficient and an upgrade is needed. The upgrade will be implemented in several stages, and from 2004 to 2005 a new software program was developed that allows recording of data in parallel. It has been operational already and has achieved a recording rate close to 40 MB/s. In 2005, a new hardware system based on a PC farm is introduced, and will be oprational in 2006 to achieve a rate of 60 MB/s. Beyond that, gradual improvements to the farm and software would bring us to close to 100 MB/s.

## 2.3 Silicon vertex trigger SVT

SVT is a hardware at the second level of the trigger system and utilizes information from the silicon vertex detector (SVX-II) and selects tracks that have large impact parameters with respect to the production point, which is approximated with the position of the Tevatron beam. The device is implemented in Run II for the first time and has been operational very successfully. It has enabled CDF to collect particles originating from decays of long-lived heavy quark hadrons such as $D$ and $B$ mesons, and to reconstruct their decays which include only hadrons in the final state, such as $\bar{B}_s^0 \to K^+K^-$ and $\bar{B} \to D\pi$.

The device also needs to be speeded up for high luminosity. A new electronics board has been developed and installed in 2004, which resulted in a 30% reduction in trigger decision time. In 2005 the development of a new hit buffer board and new algorithms is completed. T. Maruyama and M. Aoki (Tsukuba) are involved in the SVT work.

# References


[1] "Top Pair Production Cross Section in Lepton + Jets Channel with Displaced Vertex", CDF Collaboration, CDF public note 8110 (2006) ;
"Measurement of the Cross Section for $t\bar{t}$ Production in $p\bar{p}$ Collisions using the Kinematics of Lepton + Jets Events",
D. Acosta *et al*, Phys. Rev. Lett. **93**, 142001 (2004).

[2] "A Measurement of the $t\bar{t}$ Production Cross Section Using Dileptons",
CDF Collaboration, CDF public note 8103 (2006) ;
"Measurement of the $t\bar{t}$ Production Cross Section in $p\bar{p}$ Collisions at $\sqrt{s} = 1.96$ TeV Using Dilepton Events",
D. Acosta *et al*, Phys. Rev. D **72**, 052003 (2005).

[3] "Precision Top Quark Mass Measurement in the Lepton + Jets Topology in $p\bar{p}$ Collisions at $\sqrt{s} = 1.96$ TeV",
A. Abulencia *et al*, Phys. Rev. Lett. **96**, 022004 (2006).

[4] "Measurement of the Top Quark Mass with the Collider Detector at Fermilab",
Koji Sato, Ph. D. thesis, University of Tsukuba, February 2005.

[5] K. Kondo, J. Phys. Soc. Jap. **57**, 4126 (1988).

[6] "Measurement of the Top Quark Mass with the Dynamical Likelihood Method using Lepton plus Jets Events with $b$-tags in $p\bar{p}$ Collisions at $\sqrt{s} = 1.96$ TeV",
A. Abulencia *et al*, submitted to Phys. Rev. Lett. D.

[7] "Measurement of the Top Quark Mass by Dynamical Likelihood Method Using Lepton plus Jet Events in 1.96-TeV Proton-Antiproton Collisions",
Kohei Yorita, Ph. D. thesis, Waseda University, February 2005.

[8] "Measurement of the Top Quark Mass by Dynamical Likelihood Method Using Dilepton Events with the Collider Detector at Fermilab",
Ryo Tsuchiya, Ph. D. thesis, Waseda University, February 2006.

[9] "The CDF II detector, Technical design report",
CDF II Collaboration, Fermilab-Pub-96/390-E (1996).

[10] "$J/\psi$ and $\psi(2S)$ Production in $p\bar{p}$ Collisions at $\sqrt{s} = 1.8$ TeV",
CDF Collaboration, F. Abe *et al.*, Phys. Rev. Lett. **79**, 572 (1997).
"Production of $J/\psi$ from $\chi_c$ Decays in $p\bar{p}$ Collisions",
CDF Collaboration, F. Abe *et al.*, Phys. Rev. Lett. **79**, 578 (1997).

[11] "Measurement of the $J/\psi$ meson and $B$-hadron Production Cross Sections in $p\bar{p}$ Collisions at $\sqrt{s} = 1960$ GeV",
CDF Collaboration, D. Acosta *et al.*, Phys. Rev. D **71**, 032001 (2005).

[12] "Measurement of $J/\psi$ Meson and $b$-hadron Production Cross Section in Proton-Antiproton Collisions at $\sqrt{s} = 1.96$ TeV",
Tomohiro Yamashita, Ph. D. Thesis, Okayama University, January 2006.

[13] "Measurement of the $B_c$ Meson Lifetime with the Collider Detector at Fermilab",
Masato Aoki, Ph. D. Thesis, University of Tsukuba, February 2006.

[14] "Measurement of the $B$ Meson Lifetimes with the Collider Detector at Fermilab", Satoru Uozumi, Ph. D. Thesis, University of Tsukuba, July 2005.

[15] "Search for Higgs Boson Decaying to $b\bar{b}$ and Produced in Association with $W$ Bosons in $p\bar{p}$ Collisions at $\sqrt{s} = 1.96$ TeV,
A. Abulencia *et al*, Phys. Rev. Lett. **96**, 081803 (2006).

[16] "Search for Higgs Boson Production in Association with the $W$ Boson in 1.96-TeV Proton-Antiproton Collisions",
Yoshio Ishizawa, Ph. D. Thesis, University of Tsukuba, September 2005.

[17] "Search for the Higgs Boson Using High-$p_T$ Isolated Like-Sign Dilepton Events in 1.96-TeV Proton-Antiproton Collisions",
Hirokazu Kobayashi, Ph. D. Thesis, University of Tsukuba, February 2005.

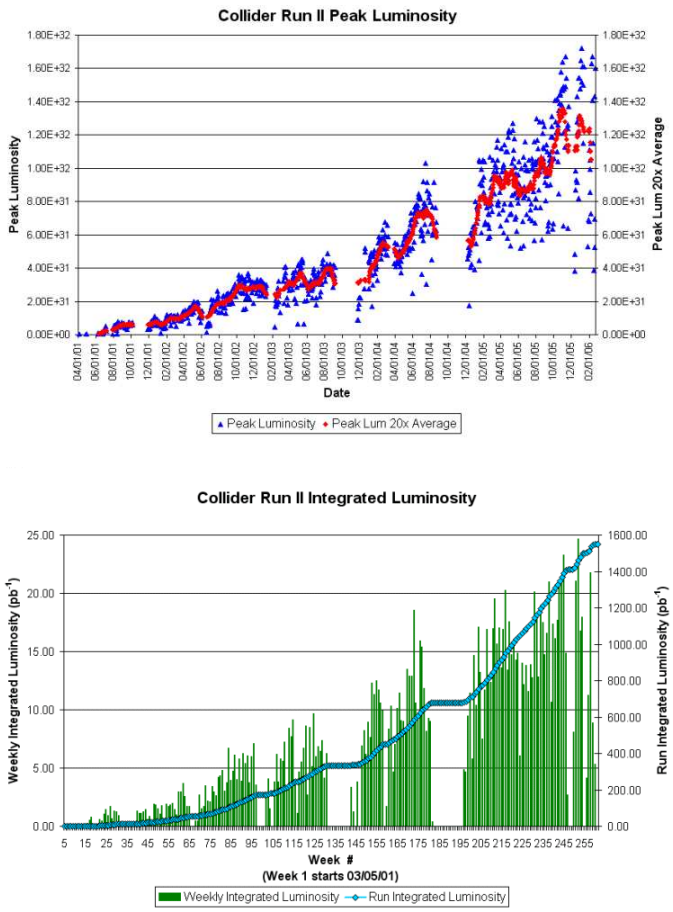


Figure 1: Tevatron performance in Run II. Top: instantaneous luminosity at the beginning of each store. Bottom: integrated luminosity delivered by week.

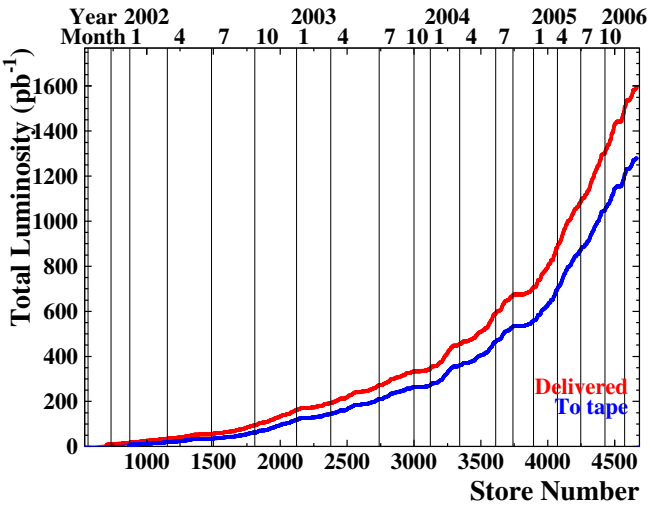


Figure 2: Integrated luminosity (top) delivered to and (bottom) recorded by CDF thus far in Tevatron Run II.

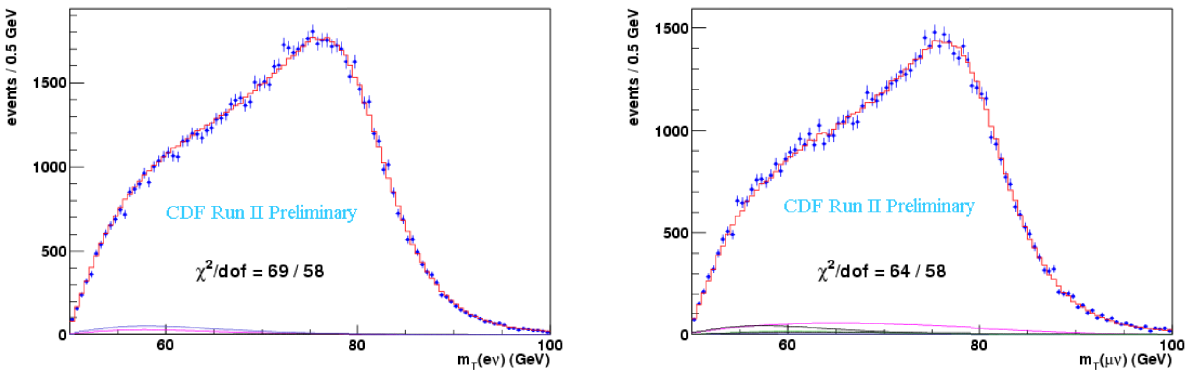


Figure 3: Transverse mass distribution of Run-II $W^{\pm} \to e^{\pm}\nu$ (left) and $\mu^{\pm}\nu$ (right) candidates.

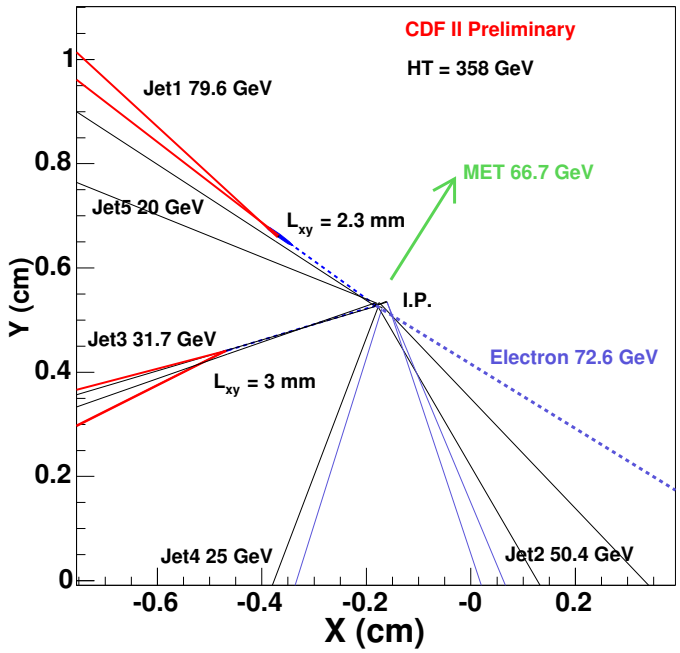


Figure 4: A top quark candidate event in the lepton + jet channel, where two $b$-jets are tagged by secondary vertices.

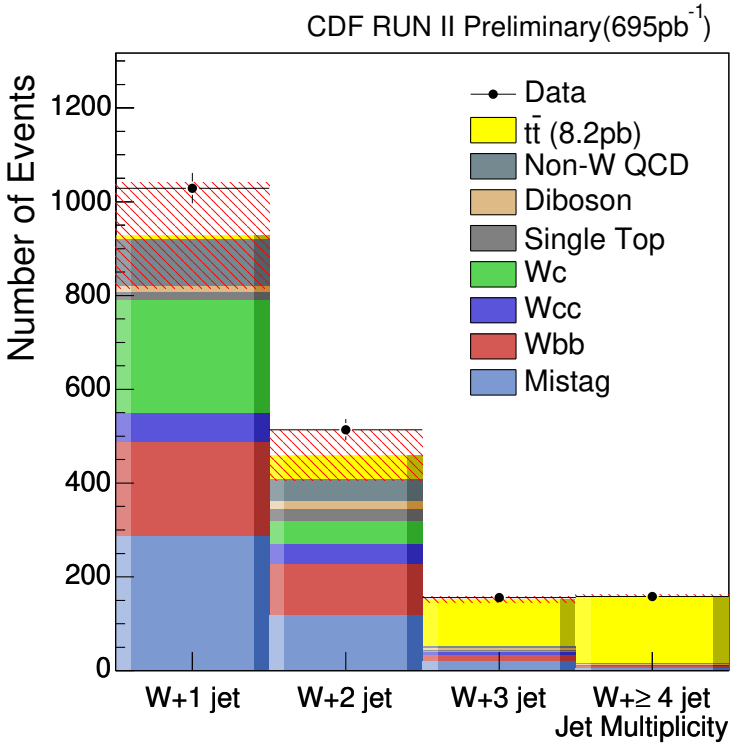


Figure 5: Multiplicity distribution of jets in $W + n$-jet events where $b$-jets are tagged with secondary vertices.

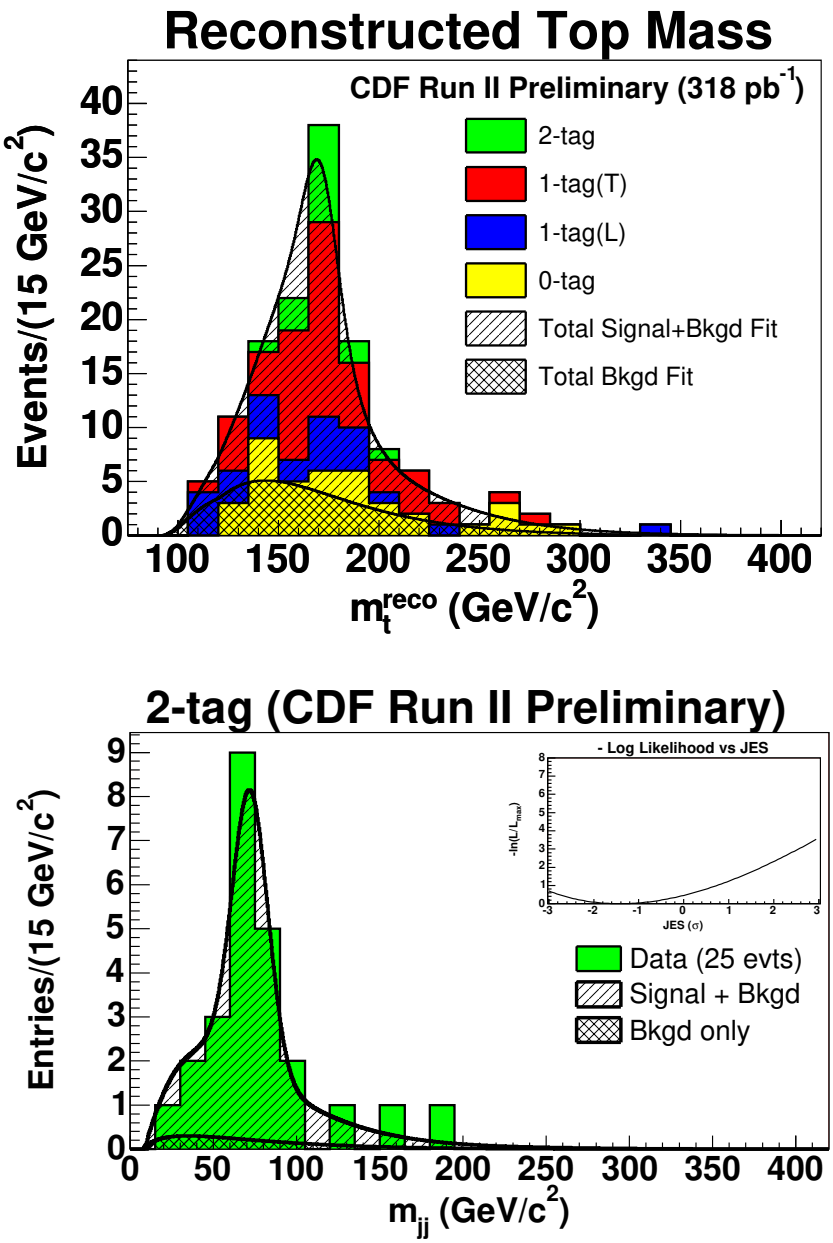


Figure 6: Top quark mass measurement from the lepton + jet channel in Run II data (320 pb$^{-1}$), with a subsample where two $b$-quark jets are tagged with secondary vertices. The top plot shows the reconstructed top quark mass distribution, while the bottom plot shows the mass distribution of the two candidate jets corresponding to $W \to q\bar{q}'$ pairs in the $t\bar{t}$ events.

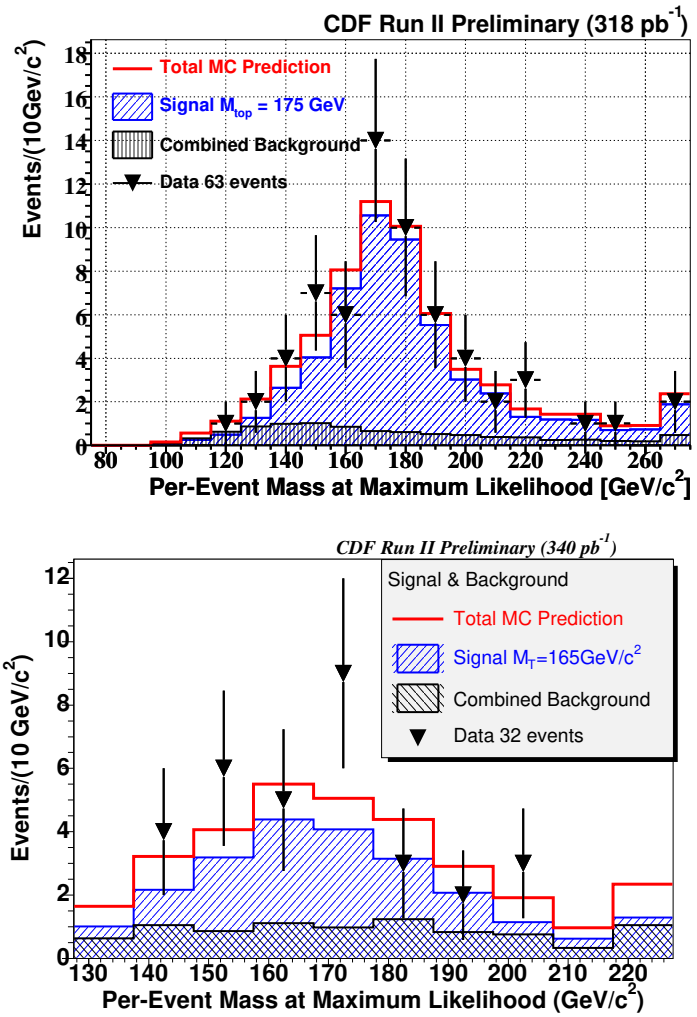


Figure 7: Top quark mass measurements using the Dynamical Likelihood Method. The maximum likelihood mass distributions are shown from the lepton + jet channel (top) and the dilepton channel (bottom).

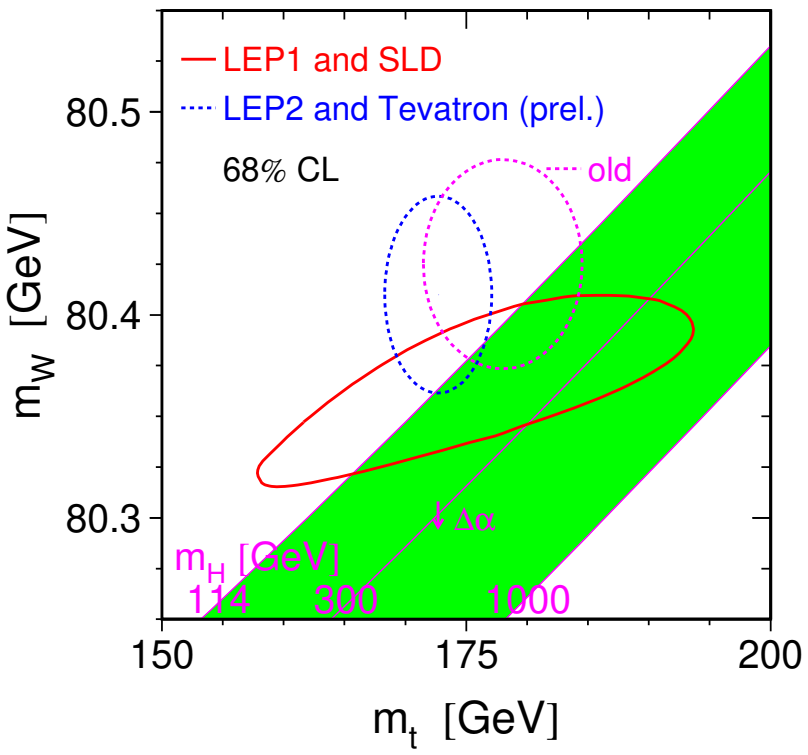


Figure 8: Measurements of the top quark and $W$ boson masses, and indirect information on the Higgs boson mass.

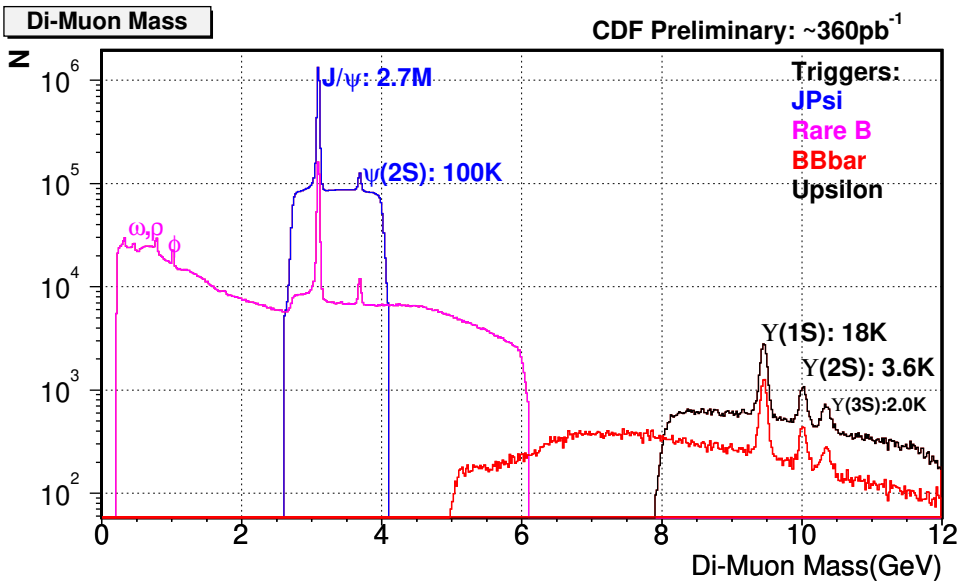


Figure 9: Invariant mass distribution of di-muon candidates. Various resonance states are seen.

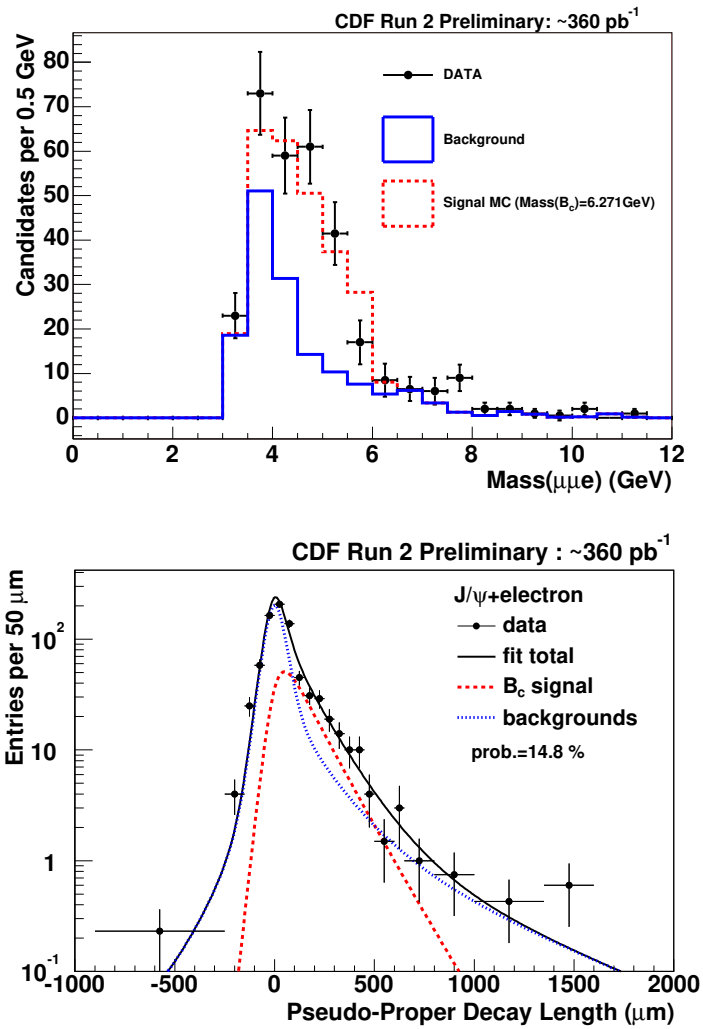


Figure 10: Measurement of the production rate and the lifetime of the $B_c^-$ meson using the semileptonic decay $B_c^- \to \ell^- \bar{\nu} J/\psi X$. Top: Electron-$J/\psi$ mass distribution. Bottom: Pseudo-proper decay length distribution of $B_c^- \to \ell^- \bar{\nu} J/\psi X$ candidates.

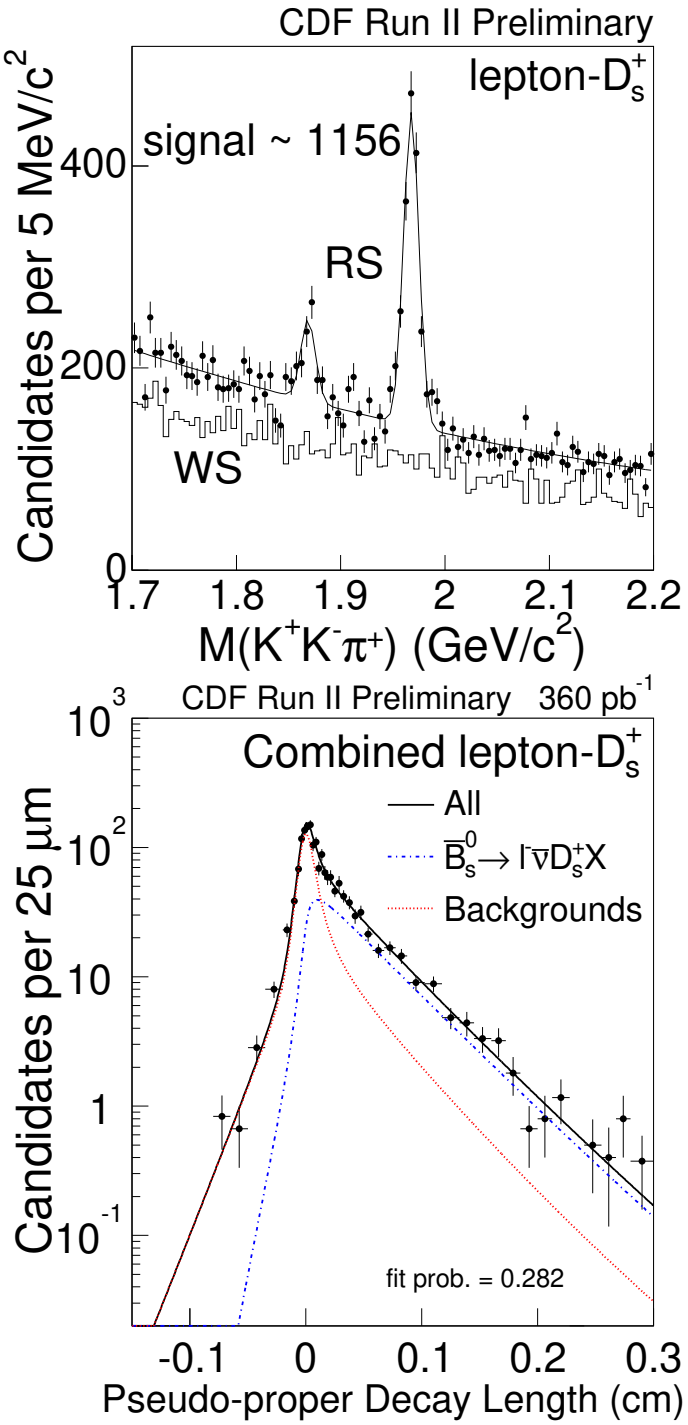


Figure 11: Measurement of the lifetime of the $B_s^-$ meson using the partially reconstructed semileptonic decays $\bar{B}_s^0 \to \ell^- \bar{\nu} D_s^+ X$. Top: Reconstructed $D_s^+ \to \phi\pi^+$ signal. Bottom: Pseudo-proper decay length distribution of $\bar{B}_s^0 \to \ell^- \bar{\nu} D_s^+ X$ candidates.

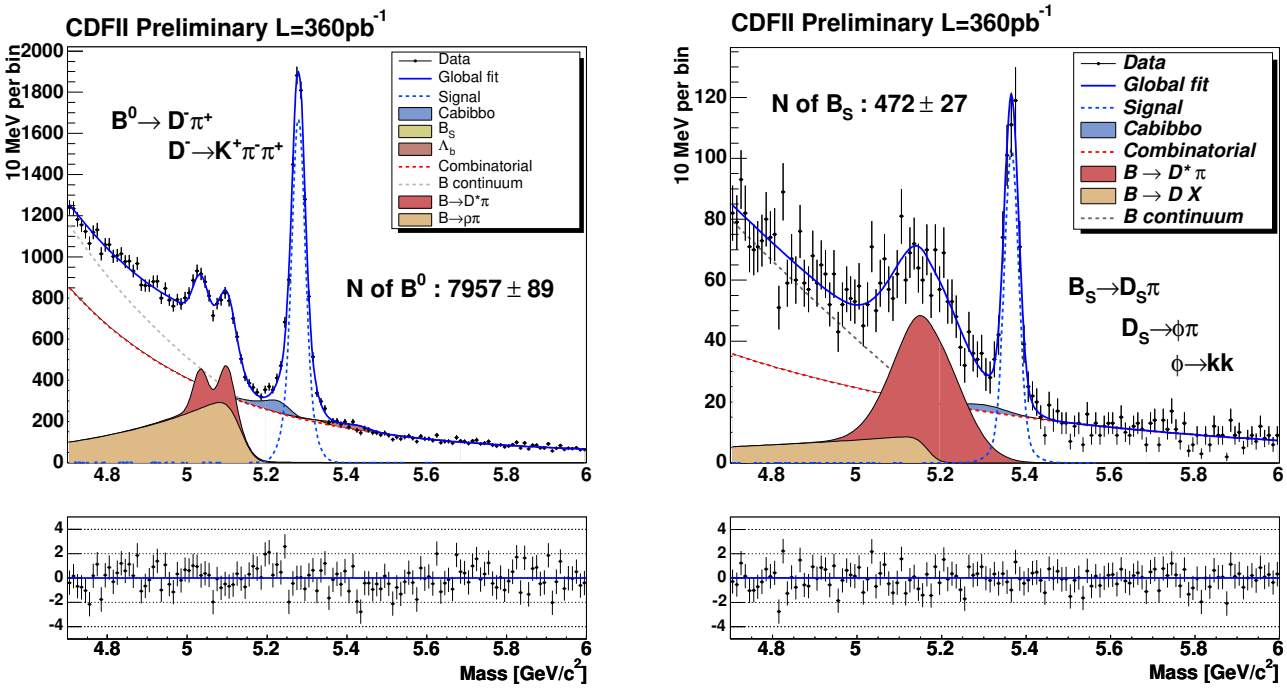


Figure 12: $B$ meson signals from SVT trigger. Left: $\bar{B}^0 \to D^+\pi^-$, $D^+ \to K^-\pi^+\pi^+$. Right: $\bar{B}_s^0 \to D_s^+\pi^-$, $D_s^+ \to \phi\pi^+$.

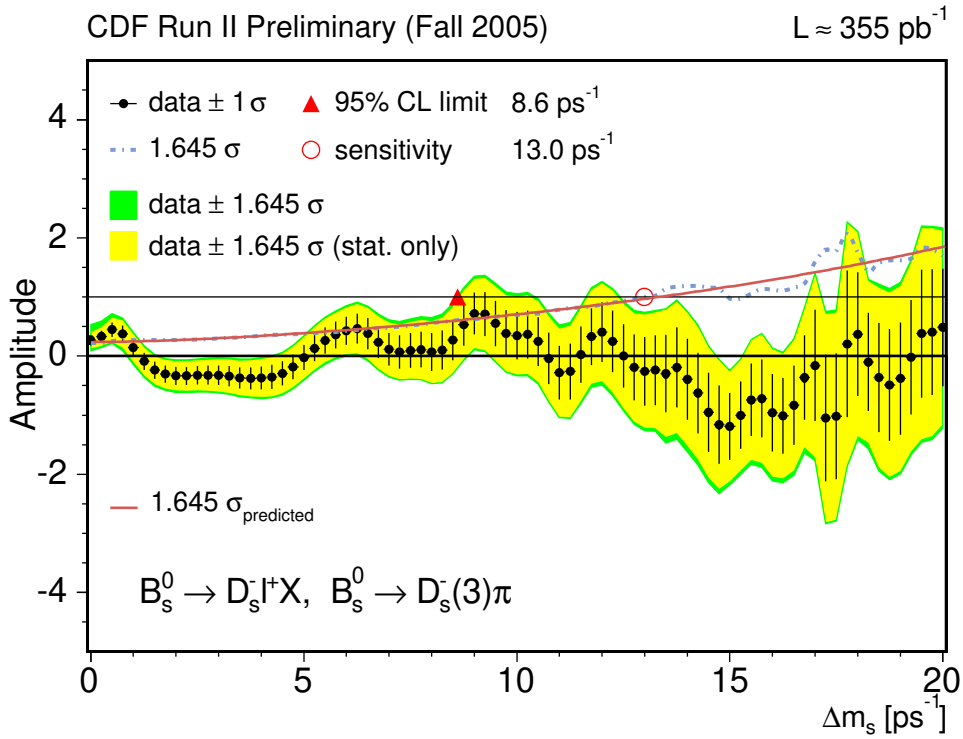


Figure 13: Search for the $B_s^0$-$\bar{B}_s^0$ oscillations. The amplitude of possible oscillations is shown as a function of the frequency $\Delta m$. The experimental data exclude the region $\Delta m_s < 8.6$ ps$^{-1}$.

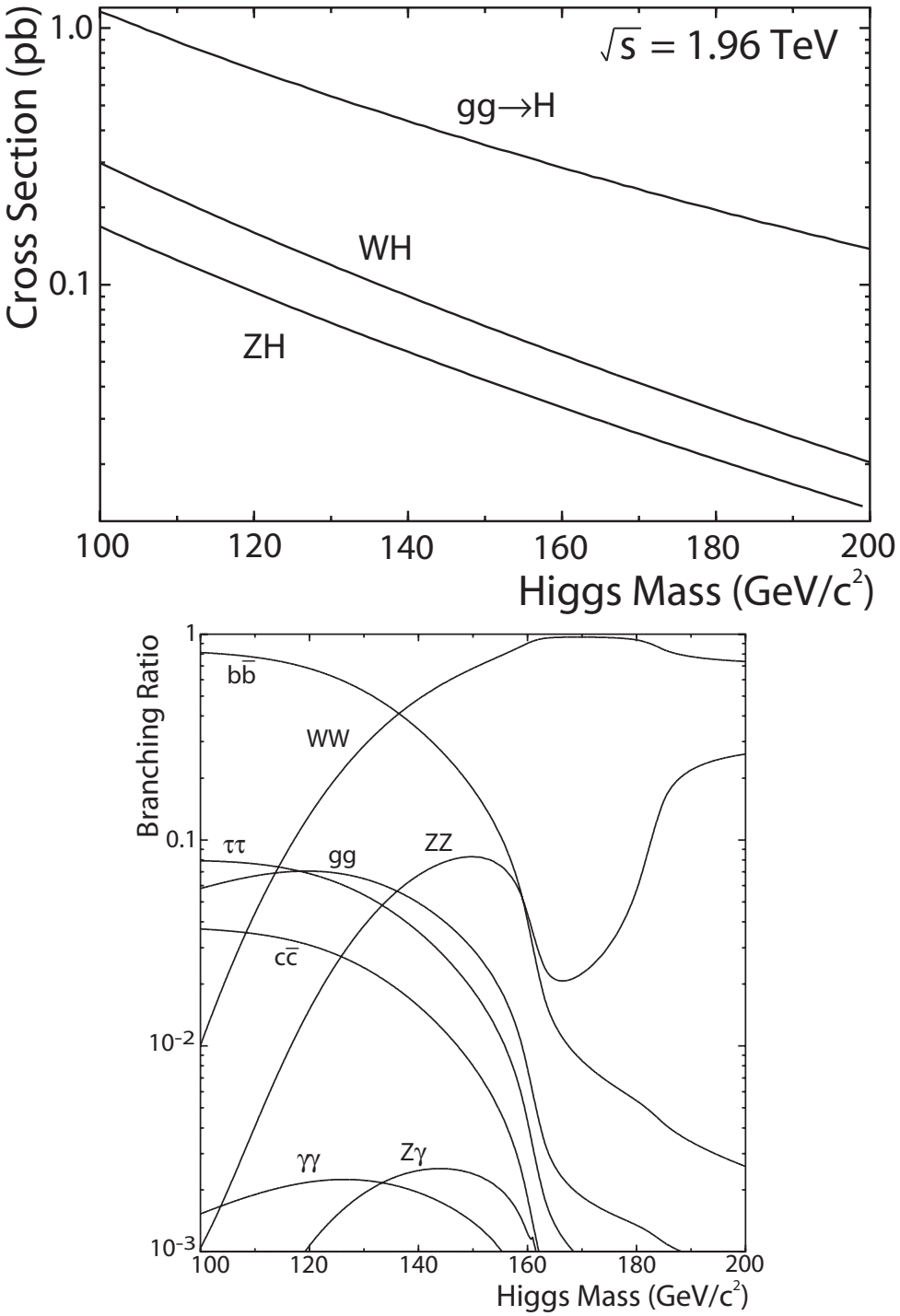


Figure 14: Top: Cross section for the production of the standard model Higgs boson at Tevatron. Bottom: Branching fractions of the standard model Higgs boson to various final states. Both plots show dependences on the Higgs boson mass.

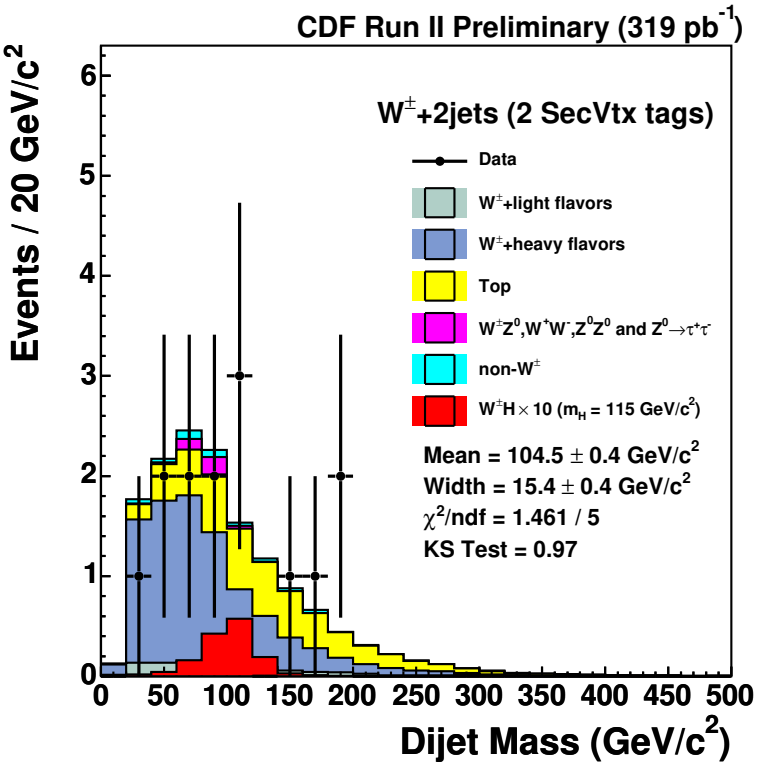


Figure 15: Invariant mass distribution of the two $b$-quark candidate jets produced in association with a $W$ boson.

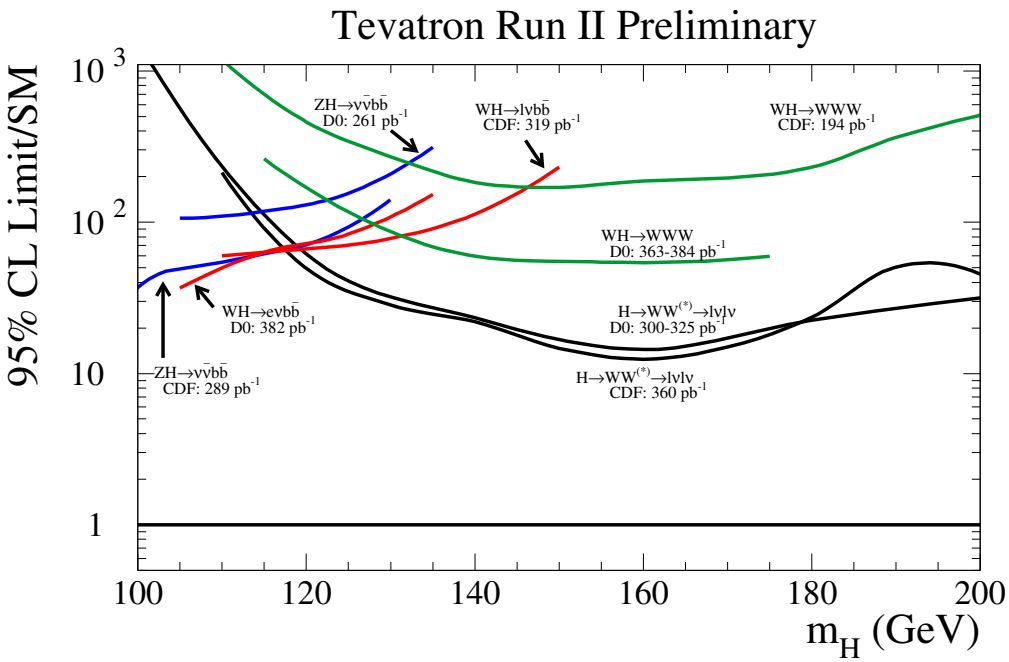


Figure 16: Summary of CDF results on the searches for the standard model Higgs boson. The experimental upper limits on production cross sections, normalized to the theoretical predictions, are shown for all search channels.